Inorganic Chemistry
Article

Inorg. Chem. **2009**, *48*, 8911–8924 **8911**
DOI: 10.1021/ic901138h

Highly Organized Structures and Unusual Magnetic Properties of Paddlewheel Copper(II) Carboxylate Dimers Containing the $\pi-\pi$ Stacking, 1,8-Naphthalimide Synthon

Daniel L. Reger,* Agota Debreczeni, Bryn Reinecke, Vitaly Rassolov, and Mark D. Smith

Department of Chemistry and Biochemistry, University of South Carolina Columbia, South Carolina 29208

Radu F. Semeniuc

Department of Chemistry, Eastern Illinois University Charleston, Illinois 61920

Received June 12, 2009

The substituted carboxylate compounds *N*-(3-propanoic acid)-1,8-naphthalimide ($\mathbf{HL_{C2}}$) and *N*-(4-butanoic acid)-1,8-naphthalimide ($\mathbf{HL_{C3}}$) react with $Cu_2(O_2CCH_3)_4(H_2O)_2$ in the presence of either pyridine (py) or 4,4′-bipyridine (bipy) to produce the dimeric complexes $[Cu_2(\mathbf{L_{C2}})_4(py)_2]\cdot 2(CH_2Cl_2)\cdot(CH_3OH)$ (**1**), $[Cu_2(\mathbf{L_{C3}})_4(py)_2]\cdot 2(CH_2Cl_2)$ (**2**), $[Cu_2(\mathbf{L_{C2}})_4(bipy)]\cdot$unknown solvent (**3**), and $[Cu_2(\mathbf{L_{C3}})_4(bipy)]\cdot(CH_3OH)_2\cdot(CH_2Cl_2)_{3.37}$ (**4**). The core of these four compounds contains the square $Cu_2(O_2CR)_4$ "paddlewheel" secondary building unit (SBU) structural motif with nonbonding Cu···Cu distances that average 2.66 Å, with each copper in a nearly square pyramidal geometry. Strong $\pi-\pi$ stacking interactions of the 1,8-naphthalimide groups organize the structures of **1** and **2** into sheets and into a three-dimensional structure for **1**. The propylene connector in the $\mathbf{L_{C3}}$ ligand allows an arrangement of the 1,8-naphthalimide groups that is different from the square shape of the SBU core. Use of the 4,4′-bipyridine linking ligand produces a three-dimensional structure for **4** organized by both covalent bonds and noncovalent forces where the 1,8-naphthalimide groups organize into a sheet structure and the 4,4′-bipyridine ligands link the sheets. In contrast, in **3**, the 1,8-naphthalimide groups overlap to form only one-dimensional ribbons, with the second dimension formed by the 4,4′-bipyridine ligands and the third dimension linked by mechanical interlocking of these two-dimensional units. Although many of the $\pi-\pi$ stacking interactions of the 1,8-naphthalimide groups are made with the dipole vectors of this group oriented at 180° (head-to-tail arrangement), skewed arrangements are observed in many cases. Ab initio calculations show that the interaction is relatively insensitive to this angle of rotation, apart from the region of steric repulsion when the rotation angle of the dipoles approaches 0°. Structural results also demonstrate that the rings can slip with respect to each other and maintain substantial interactions. These highly organized, extended structures influence the magnetic properties where all four compounds are strongly antiferromagnetically coupled, leading to diamagnetic Cu(II) solids at and above room temperature with *J* values that must be more negative than -600 cm^{-1}.

Introduction

Crystal engineering is a topic of intense research interest that holds promise for revolutionizing materials design and synthesis. While promising results have been achieved and startling applications are being developed,[1] much work is still needed to lay a foundation for a unified supramolecular theory[2] with practical applications in the field of crystal engineering. A crucial step along the path to predicting solid structures from the substituent groups of the chemical species of interest is to better understand the factors that govern the noncovalent assembly of molecules or ions into solid state architectures. Remarkable strides have been made with both common organic and inorganic systems as has been the subject of several reviews.[3]

The essential key is the identification of reliable, robust supramolecular synthons that can be transferred from one system to another. Hydrogen bonding is a widely used tool in crystal engineering because the directionality and strength of its associative protocol enables easy and reliable transfer to other systems.[4] In contrast, $\pi-\pi$ stacking is generally a weaker force and has a less predictable directional associative protocol, because variable orientations of the involved moieties often occur in order to maximize the electrostatic attraction between the σ framework and the π electron density of the stacked groups.[5] Although association of

*To whom correspondence should be addressed. E-mail: reger@mail.chem.sc.edu.

Published on Web 08/21/2009

several π species in solution has been substantiated in some cases, little is known about their solution structure and their relative orientation.[6]

It has long been established that the order of stability in the interaction of two π systems is π-deficient$-\pi$-deficient > π-deficient$-\pi$-rich > π-rich$-\pi$-rich.[5] We have recently incorporated a π-deficient functionality, a 1,8-naphthalimide group (Scheme 1), into bis(pyrazolyl)methane and 2,2′-bipyridine systems of ligands and shown that several metal complexes of these ligands have a common feature: a $\pi-\pi$ stacking interaction with the dipole vectors (which run from the center of the fused aromatic group through the nitrogen atom, red arrow, Scheme 1) of the 1,8-naphthalimide groups oriented at 180°, antiparallel.[7] Thus, we have shown that it is possible to design, synthesize, and implement strong, directional $\pi-\pi$ stacking for crystal engineering, because the 1,8-naphthalimide group leads to association into dimers of

Scheme 1. The 1,8-Naphthalimide Group[a]

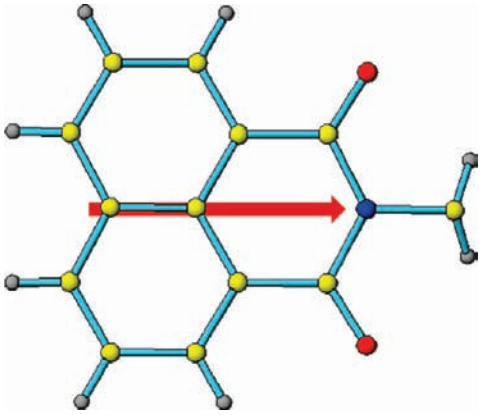

[a] The red arrow represents the dipole moment. Color code: carbon, yellow; oxygen, red; nitrogen, blue; hydrogen, gray.

metal complexes of the ligands in both solution and the solid state, as evidenced by electrospray mass spectrometry, pulsed-field gradient spin echo NMR spectroscopy techniques and X-ray diffraction experiments.

We desired to use this strong $\pi-\pi$ stacking interaction of the 1,8-naphthalimide group in the synthesis of metal organic frameworks (MOFs). In this area, three overlapping synthetic approaches are followed: reticular synthesis,[8] ligand-to-metal coordination,[9] and supramolecular assembly.[10] Reticular synthesis can be described as the process of assembling judiciously designed, rigid molecular building blocks into predetermined ordered structures (networks), which are held together by strong bonding forces. Multidentate linkers such as carboxylates have been used for the formation of rigid MOFs via reticular synthesis due to their ability to aggregate metal ions into neutral clusters, referred to as secondary building units (SBUs). The SBUs are rigid because the metal ions are locked into their positions by the carboxylates; thus, the SBUs serve as large rigid vertices that can be joined by

(1) (a) DeIonno, E.; Tseng, H.-R.; Harvey, D. D.; Stoddart, J. F.; Heath, J. R. *J. Phys. Chem. B* **2006**, *110*, 7609. (b) Moonen, N. N. P.; Flood, A. H.; Fernandez, J. M.; Stoddart, J. F. *Top. Curr. Chem.* **2005**, *262*, 99. (c) Collin, J.-P.; Heitz, V.; Sauvage, J.-P. *Top. Curr. Chem.* **2005**, *262*, 29. (d) Balzani, V.; Credi, A.; Ferrer, B.; Silvi, S.; Venturi, M. *Top. Curr. Chem.* **2005**, *262*, 1. (e) Balzani, V.; Clemente-Leon, M.; Credi, A.; Ferrer, B.; Venturi, M.; Flood, A. H.; Stoddart, J. F. *Proc. Natl. Acad. Sci. U.S.A.* **2006**, *103*, 1178. (f) Saha, S.; Johansson, E.; Flood, A. H.; Tseng, H.-R.; Zink, J. I.; Stoddart, J. F. *Chem.—Eur. J.* **2005**, *11*, 6846. (g) Liu, Y.; Flood, A. H.; Bonvallet, P. A.; Vignon, S. A.; Northrop, B. H.; Tseng, H.-R.; Jeppesen, J. O.; Huang, T. J.; Brough, B.; Baller, M.; Magonov, S.; Solares, S. D.; Goddard, W. A.; Ho, C.-M.; Stoddart, J. F. *J. Am. Chem. Soc.* **2005**, *127*, 9745. (h) Badjic, J. D.; Balzani, V.; Credi, A.; Silvi, S.; Stoddart, J. F. *Science* **2004**, *303*, 1845. (i) Hernandez, R.; Tseng, H.-R.; Wong, J. W.; Stoddart, J. F.; Zink, J. I. *J. Am. Chem. Soc.* **2004**, *126*, 3370. (j) Kay, E. R.; Leigh, D. A. *Top. Curr. Chem.* **2005**, *262*, 133. (k) Tian, H.; Wang, Q.-C. *Chem. Soc. Rev.* **2006**, *35*, 361. (l) Yoshizawa, M.; Miyagi, S.; Kawano, M.; Ishiguro, K.; Fujita, M. *J. Am. Chem. Soc.* **2004**, *126*, 9172. (m) Yoshizawa, M.; Takeyama, Y.; Kusukawa, T.; Fujita, M. *Angew. Chem., Int. Ed.* **2002**, *41*, 1347. (n) Fiedler, D.; Bergman, R. G.; Raymond, K. N. *Angew. Chem., Int. Ed.* **2004**, *43*, 6748.

(2) (a) Khlobystov, A. N.; Blake, A. J.; Champness, N. R.; Lemenovskii, D. A.; Majouga, G.; Zyk, N. V.; Schroder, M. *Coord. Chem. Rev.* **2001**, *222*, 155. (b) Blake, A. J.; Champness, N. R.; Hubberstey, P.; Li, W. S.; Withersby, M. A.; Schroder, M. *Coord. Chem. Rev.* **1999**, *183*, 117. (c) Blake, A. J.; Baum, G.; Champness, N. R.; Chung, S. S. M.; Cooke, P. A.; Fenske, D.; Khlobystov, A. N.; Lemenovskii, D. A.; Li, W.-S.; Schroder, M. *J. Chem. Soc., Dalton Trans.* **2000**, 4285. (d) Abourahma, H.; Bodwell, G. J.; Lu, J.; Moulton, B.; Pottie, I. R.; Bailey, W. R; Zaworotko, M. J. *Cryst. Growth Des.* **2003**, *3*, 513. (e) Bourne, S. A.; Mondal, A.; Zaworotko, M. *J. Cryst. Eng.* **2001**, *4*, 25. (f) Moulton, B.; Zaworotko, M. *J. Chem. Rev.* **2001**, *101*, 1629. (g) Lu, J.; Moulton, B.; Zaworotko, M. J.; Bourne, S. A. *Chem. Comm.* **2001**, 861.

(3) (a) Braga, D.; Brammer, L.; Champness, N. R. *Cryst. Eng. Comm.* **2005**, *7*, 1. (b) Brammer, L. *Chem. Soc. Rev.* **2004**, *33*, 476. (c) James, S. *Chem. Soc. Rev.* **2003**, *32*, 276. (d) Janiak, C. *J. Chem. Soc., Dalton Trans.* **2003**, 2781. (e) Sharma, C. V. K. *Cryst. Growth Des.* **2002**, *2*, 465. (f) Lee, S. J.; Lin, W. *Acc. Chem. Res.* **2007**, *41*, 521. (g) Ma, L.; Lee, J. Y.; Li, J.; Lin, W. *Inorg. Chem.* **2008**, *47*, 3955.

(4) (a) Braga, D.; Maini, L.; Polito, M.; Tagliavini, E.; Grepioni, F. *Coord. Chem. Rev.* **2003**, *53*, 246. (b) Desiraju, G. R. *Acc. Chem. Res.* **2002**, *35*, 565. (c) Moulton, B.; Zaworotko, M. *J. Chem. Rev.* **2001**, *101*, 1629. (d) Desiraju, G. R. *J. Chem. Soc., Dalton Trans.* **2000**, 3745. (e) Braga, D.; Grepioni, F. *Acc. Chem. Res.* **2000**, *33*, 601. (f) Beatty, A. M. *Coord. Chem. Rev.* **2003**, *246*, 131. (g) Brammer, L. *Chem. Soc. Rev.* **2004**, *33*, 476. (h) Brammer, L. *J. Chem. Soc., Dalton Trans.* **2003**, 3145.

(5) Janiak, C. *J. Chem. Soc., Dalton Trans.* **2000**, 3885 and references therein.

(6) (a) Olenik, B.; Boese, R.; Sustmann, R. *Cryst. Growth Des.* **2003**, *3*, 175. (b) Garcia-Baez, E. V.; Martinez-Martinez, F. J.; Hoepfl, H.; Padilla-Martinez, I. I. *Cryst. Growth Des.* **2003**, *3*, 35. (c) Noveron, J. C.; Lah, M. S.; Del Sesto, R. E.; Arif, A. M.; Miller, J. S.; Stang, P. J. *J. Am. Chem. Soc.* **2002**, *124*, 6613. (d) Marsden, J. A.; Miller, J. J.; Shirtcliff, L. D.; Haley, M. M. *J. Am. Chem. Soc.* **2005**, *127*, 2464.

(7) (a) Reger, D. L.; Elgin, J. D.; Semeniuc, R. F.; Pellechia, P. J.; Smith, M. D. *Chem. Comm.* **2005**, 4068. (b) Reger, D. L.; Semeniuc, R. F.; Elgin, J. D.; Rassolov, V.; Smith, M. D. *Cryst. Growth Des.* **2006**, *6*, 2758. (c) Reger, D. L.; Elgin, J. D.; Smith, M. D; Simpson, B. K. *Polyhedron* **2009**, *28*, 1469.

(8) (a) Sudik, A. C.; Cote, A. P.; Wong-Foy, A. G.; O'Keeffe, M.; Yaghi, O. M. *Angew. Chem., Int. Ed.* **2006**, *45*, 2528. (b) Stallmach, F.; Groeger, S.; Kuenzel, V.; Kaerger, J.; Yaghi, O. M.; Hesse, M.; Mueller, U. *Angew. Chem., Int. Ed.* **2006**, *45*, 2123. (c) Wong-Foy, A. G.; Matzger, Adam, J.; Yaghi, O. M. *J. Am. Chem. Soc.* **2006**, *128*, 3494. (d) Rowsell, J. C.; Yaghi, O. M. *J. Am. Chem. Soc.* **2006**, *128*, 1304. (e) Spencer, E. C.; Howard, J. K.; McIntyre, G. J.; Rowsell, J. C.; Yaghi, O. M. *Chem. Comm.* **2006**, 278. (f) Millward, A. R.; Yaghi, O. M. *J. Am. Chem. Soc.* **2005**, *127*, 17998. (g) Rowsell, J. C.; Eckert, J.; Yaghi, O. M. *J. Am. Chem. Soc.* **2005**, *127*, 14904. (h) Ni, Z.; Yassar, A.; Antoun, T.; Yaghi, O. M. *J. Am. Chem. Soc.* **2005**, *127*, 12752. (i) Rowsell, J. C.; Spencer, E. C.; Eckert, J.; Howard, J. K.; Yaghi, O. M. *Science* **2005**, *309*, 1350. (j) Chen, B.; Ockwig, N. W.; Millward, A. R.; Contreras, D. S.; Yaghi, O. M. *Angew. Chem., Int. Ed.* **2005**, *44*, 4745. (k) Rowsell, J. L. C.; Yaghi, O. M. *Angew. Chem., Int. Ed.* **2005**, *44*, 4670. (l) Yaghi, O. M.; O'Keeffe, M.; Ockwig, N. W.; Chae, H. K.; Eddaoudi, M.; Kim, J. *Nature* **2003**, *423*, 705. (m) Eddaoudi, M.; Moler, D. B.; Li, H.; Chen, B.; Reineke, T. M.; O'Keeffe, M.; Yaghi, O. M. *Acc. Chem. Res.* **2001**, *34*, 319. (n) O'Keeffe, M.; Eddaoudi, M.; Li, H.; Reineke, T.; Yaghi, O. M. *J. Solid State Chem.* **2000**, *152*, 3. (o) Moulton, B.; Zaworotko, M. J. *Curr. Opin. Solid State Mater. Sci.* **2002**, *6*, 117. (p) Moulton, B.; Zaworotko, M. *J. Chem. Rev.* **2001**, *101*, 1629. (q) Zaworotko, M. J. *Angew. Chem., Int. Ed.* **2000**, *39*, 3052.

(9) (a) Robson, R. *J. Chem. Soc., Dalton Trans.* **2008**, 5113. (b) Murray, L. J.; Dinca, M.; Long, J. R. *Chem. Soc. Rev.* **2009**, *38*, 1294. (c) Perry, J. J.; Perman, J. A.; Zaworotko, M. J. *Chem. Soc. Rev.* **2009**, *38*, 1400.

(10) (a) Lehn, J. M. *Chem. Scr.* **1988**, *28*, 237−262. (b) Liu, C.-S.; Wang, J.-J.; Yan, L.-F.; Chang, Z.; Bu, X.-H.; Sanudo, E. C.; Ribas, J. *Inorg. Chem.* **2007**, *46*, 6299. (c) Li, X.-P.; Pan, M.; Zheng, S.-R.; Liu, Y.-R.; He, Q.-T.; Kang, B.-S.; Su, C.-Y. *Cryst. Growth Des.* **2007**, *7*, 2481. (d) Wang, C.-C.; Tseng, S.-M.; Lin, S.-Y.; Liu, F.-C.; Dai, S.-C.; Lee, G.-H.; Shih, W.-J.; Sheu, H.-S. *Cryst. Growth Des.* **2007**, *7*, 1783. (e) Wang, X.-L.; Bi, Y.-F.; Liu, G.-C.; Lin, H.-Y.; Hu, T.-L.; Bu, X.-H. *Cryst. Eng. Comm.* **2008**, *10*, 349.

robust organic links to produce extended frameworks of high structural stability.

Ligand-to-metal coordination (using mostly rigid pyridine-based ligands) is widely used in the formation of similar coordination polymers containing large voids, usually filled with solvent molecules.[9] These species can be viewed as different from those obtained using reticular synthesis in that, in some cases, the stability of the MOFs is reduced, and the network collapses upon the removal of solvent molecules.[3c,d,8] A third approach, supramolecular assembly,[10] consists of utilizing noncovalent interactions (such as hydrogen bonding and $\pi-\pi$ stacking) to assemble the framework, in this case, the structural stability of the assembly being the most fragile.[11]

Reported here are results obtained by preparing ligands that contain both the carboxylate and the 1,8-naphthalimide group, a group we have shown to enter into strong $\pi-\pi$ stacking interactions, for the synthesis of new complexes built around the copper carboxylate dimer core, using pyridine ligands as the axial group. *This unique synthetic approach combines all three of the methods described above*: the reticular synthesis based on carboxylate groups, the ligand-to-metal coordination of rigid pyridine-based ligands, and the strong $\pi-\pi$ stacking interactions of the 1,8-naphthalimide group. As such, we anticipated the formation of neutral MOFs of the formula $Cu_2(O_2CR)_4(pyridine)_2$ with architectures that are usually associated with reticular synthesis yet organize in at least one dimension using the (supramolecular) directional, noncovalent $\pi-\pi$ association algorithm of the 1,8-naphthalimide moieties. We have chosen the copper carboxylate system, from a variety of possible SBUs,[12] for three main reasons. First, we wanted the "square" architecture offered by the paddlewheel shape, an architecture that we planned to manipulate by changing the length of the link between the carboxylate and 1,8-naphthalimide group in our ligands. Second, we desired to have the strong axial ligation provided by this system in order to build framework solids using both terminal axial ligands, such as pyridine, and compare the structures and properties of those solids to those that form using linking ligands, such as 4,4′-bipyridine. Third, we were interested in determining the impact of highly organized supramolecular structures on the magnetic properties of copper carboxylate dimers. These types of complexes are known to exhibit strong antiferromagnetic properties.[12]

Experimental Section

General Considerations. All reactants were used as purchased from Aldrich. The ^{1}H NMR spectra were recorded on a Varian Mercury VX 300 spectrometer; the chemical shifts are reported in parts per million and are referenced to the protonated solvent residual. The ^{13}C NMR spectra were recorded on a Bruker Avance DRX 400 spectrometer, and the chemical shifts in parts per million were referenced to a residual deuterated solvent signal. Mass spectrometric measurements were obtained on a VG 70S instrument. Elemental analyses were performed by Robertson Microlit Laboratories (Madison, NJ). The reflectance measurements were done on a Perkin-Elmer Lambda 35 UV−vis spectrometer using the Labsphere RSA-PE-20 reflectance spectroscopy accessory. Microcrystalline samples were used in a 2 nm slit/4 nm cell. The magnetic properties were measured using a Quantum Design MPMSXL superconducting quantum interference magnetometer. Gelatin capsules were used as sample containers that make a negligible contribution to the overall magnetization. Complexes **1** and **2** were both warmed and cooled between 5 and 300 K in an applied field of 4 T and 0.7 T, respectively. Subsequently, complex **2** was warmed and cooled between 200 and 400 K in an applied field of 0.7 T. Complexes **3** and **4** were treated similarly between 5 and 300 K in a field of 1 T.

Synthesis of *N*-(3-Propanoic Acid)-1,8-naphthalimide (HL_{C2}). A mixture of 1,8-naphthalic anhydride (1.98 g, 10 mmol) and 3-aminopropanoic acid (0.89 g, 10 mmol) was heated at reflux in dimethylformamide (100 mL) overnight. Upon addition of the hot reaction mixture to ice and cold water, the product, $\mathbf{HL_{C2}}$, precipitated. The resulting precipitate was filtered, washed with diethylether, and air-dried to yield 2.40 g (8.9 mmol, 89%) of a white solid. Anal. Calcd (Found) for $C_{15}H_{11}O_4N$: C, 66.91 (66.71); H, 4.12 (3.98); N, 5.20 (5.40). HRMS calcd. for $C_{15}H_{11}O_4N$: 269.0688. Found: 269.0691. ^{1}H NMR ($CDCl_3$, 300 MHz): δ 8.63 (d, $J = 7.5$ Hz, 2H, napht), 8.24 (d, $J = 8.4$ Hz, 2H, napht), 7.78 (t, $J = 7.5$ Hz, 2H, napht), 4.53 (t, $J = 7.5$ Hz, 2H, N−CH_2), 2.85 (t, $J = 7.5$ Hz, 2H, CH_2−COOH). ^{13}C NMR (DMSO-d_6, 100 MHz): δ 172.5 (*C*OOH), 163.3 (C=O), 134.4, 131.3, 130.7, 127.4, 127.2, 122.0 (arene), 35.7, 32.2 (*C*H_2).

Synthesis of *N*-(4-Butanoic Acid)-1,8-naphthalimide (HL_{C3}). A mixture of 1,8-naphthalic anhydride (1.98 g, 10 mmol) and 4-aminobutanoic acid (1.03 g, 10 mmol) was heated at reflux in dimethylformamide (100 mL) overnight. Upon addition of the hot reaction mixture to ice and cold water, the product, $\mathbf{HL_{C3}}$, precipitated. The resulting precipitate was filtered, washed with diethylether, and air-dried to yield 2.71 g (9.6 mmol, 96%) of a white solid. Anal. Calcd. (Found) for $C_{16}H_{13}O_4N$: C, 67.84 (67.62); H, 4.63 (4.24); N, 4.94 (4.93). HRMS calcd. for $C_{16}H_{13}O_4N$: 283.0845. Found: 283.0841. ^{1}H NMR ($CDCl_3$, 300 MHz): δ 8.61 (dd, $J = 7.2$ Hz, $J = 1.2$ Hz, 2H, napht), 8.22 (dd, $J = 8.1$ Hz, $J = 1.2$ Hz, 2H, napht), 7.76 (dd, $J = 8.1$ Hz, $J = 7.5$ Hz, 2H, napht), 4.27 (t, $J = 6.9$ Hz, 2H, N−CH_2), 2.47 (t, $J = 7.5$ Hz, 2H, CH_2−COOH), 2.09 (quint, $J = 7.2$ Hz, 2H, CH_2−CH_2−CH_2). ^{13}C NMR (DMSO-d_6, 100 MHz): δ 174.0 (*C*OOH), 163.5 (C=O), 134.2 (*C*H arene), 131.2 (*C* arene), 130.6 (*C*H arene), 127.4 (*C* arene), 127.1 (*C*H arene), 122.1 (*C* arene), 31.3 (*C*H_2−COOH), 23.0 (CH_2−*C*H_2−CH_2). In the ^{13}C NMR spectrum, the N−*C*H_2 signal is overlapped by the DMSO-d_6 septet. The presence of a N−*C*H_2 signal was demonstrated in a gradient HMQC experiment.

Synthesis of $[Cu_2(L_{C2})_4(py)_2]\cdot 2(CH_2Cl_2)\cdot(CH_3OH)$ (1). $\mathbf{HL_{C2}}$ (0.054 g, 0.20 mmol) was dissolved in dichloromethane (20 mL) containing 10 drops of pyridine. $Cu_2(O_2CCH_3)_4(H_2O)_2$ (0.020 g, 0.050 mmol) was dissolved in methanol (20 mL). These solutions were filtered, and equal aliquots of each solution were divided into three test tubes with a buffer layer of pure methanol placed between the two solutions. After a few days, X-ray-quality crystals were obtained. Yield: 0.0266 g (0.016 mmol, 33%). Anal. Calcd. (Found) for $C_{73}H_{58}Cl_4Cu_2N_6O_{17}$: C, 56.20 (57.33); H, 3.75 (3.35); N, 5.39 (5.26). The reflectance spectrum shows two bands having maxima at 384 nm (band II) and 714 nm (band I).

Synthesis of $[Cu_2(L_{C3})_4(py)_2]\cdot 2(CH_2Cl_2)$ (2). $\mathbf{HL_{C3}}$ (0.057 g, 0.20 mmol) was dissolved in dichloromethane (20 mL) containing 10 drops of pyridine. $Cu_2(O_2CCH_3)_4(H_2O)_2$ (0.020 g,

(11) (a) Suh, M. P.; Cheon, Y. E.; Lee, E. Y. *Coord. Chem. Rev.* **2008**, *252*, 1007. (b) Przychodzen, P.; Korzeniak, T.; Podgajny, R.; Sieklucka, B. *Coord. Chem. Rev.* **2006**, *250*, 2234. (c) Yao, Q.-X.; Ju, Z.-F.; Li, W.; Wu, W.; Zheng, S.-T.; Zhang, J. *Cryst. Eng. Comm.* **2008**, *10*, 1299. (d) Carlucci, L.; Ciani, G.; Maggini, S.; Proserpio, D. M. *Cryst. Growth Des.* **2008**, *8*, 162. (e) Song, J.-F.; Lu, J.; Chen, Y.; Liu, Y.-B.; Zhou, R.-S.; Xu, X.-Y.; Xu, J.-Q. *Inorg. Chem. Commun.* **2006**, *9*, 1079.

(12) (a) Cotton, F. A.; Wilkinson, G; Murillo, C. A.; Bochmann, M. *Advanced Inorganic Chemistry*; John Wiley & Sons, Inc.: New York, 1999; pp 870−871. (b) Kahn, O. *Molecular Magnetism*; VCH Publishers, Inc.: New York, 1993. (c) Yougme, S.; Cheansirisomboon, A.; Danvirutai, C.; Pakawatchai, C.; Chaichit, N.; Engkagul, C.; van Albada, G.; Costa, J. S.; Reedijk, J. *Polyhedron* **2008**, *27*, 1875. (d) Kato, M; Muto, Y. *Coord. Chem. Rev.* **1988**, *92*, 45. (e) Melnik, M. *Coord. Chem. Rev.* **1982**, *42*, 259.

0.050 mmol) was dissolved in methanol (20 mL). These solutions were filtered, and equal aliquots of each solution were divided into three test tubes with a buffer layer of pure methanol placed between the two solutions. After a few days, X-ray-quality crystals were obtained. Yield: 0.0396 g (0.025 mmol, 50%). The analytical sample was dried to a constant weight. Anal. Calcd. (Found) for $C_{74}H_{58}Cu_2N_6O_{16}$ (without solvent): C, 62.84 (62.15); H, 4.13 (3.41); N, 5.94 (5.91). The reflectance spectrum shows two bands having maxima at 384 nm (band II) and 732 nm (band I).

Synthesis of $[Cu_2(L_{C2})_4(4,4'\text{-bipy})]\cdot$unknown solvate (3). HL_{C2} (0.054 g, 0.20 mmol) was dissolved in dichloromethane (20 mL); then, 10 drops of triethylamine and 4,4′-bipyridine (0.020 g, 0.13 mmol) dissolved in 1 mL of dichloromethane were added. $Cu_2(O_2CCH_3)_4(H_2O)_2$ (0.020 g, 0.050 mmol) was dissolved in methanol (20 mL). These solutions were filtered, and equal aliquots of each solution were divided into three test tubes with a buffer layer of pure methanol placed between the two solutions. After five days, X-ray-quality crystals were obtained. Yield: 0.013 g (0.010 mmol, 19%). The analytical sample was dried to a constant weight. Anal. Calcd. (Found) for $C_{70}H_{48}Cu_2N_6O_{16}$ (without solvent): C, 61.99 (61.81); H, 3.57 (3.09); N, 6.20 (6.13). The reflectance spectrum shows two bands having maxima at 371 nm (band II) and 753 nm (band I).

Synthesis of $[Cu_2(L_{C3})_4(4,4'\text{-bipy})]\cdot(CH_3OH)_2\cdot(CH_2Cl_2)_{3.37}$ (4). HL_{C3} (0.057 g, 0.20 mmol) was dissolved in dichloromethane (20 mL); then, 10 drops of triethylamine and 4,4′-bipyridine (0.020 g, 0.13 mmol) dissolved in 1 mL of dichloromethane were added. $Cu_2(O_2CCH_3)_4(H_2O)_2$ (0.020 g, 0.050 mmol) was dissolved in methanol (20 mL). These solutions were filtered, and equal aliquots of each solution were divided into three test tubes with a buffer layer of pure methanol placed between the two solutions. After three weeks, X-ray-quality crystals were obtained. Yield: 0.030 g (0.017 mmol, 32%). The analytical sample was dried to a constant weight. Anal. Calcd. (Found) for $C_{74}H_{56}Cu_2N_6O_{16}$ (without solvent): C, 62.93 (61.86); H, 4.00 (3.34); N, 5.95 (5.93). The reflectance spectrum shows two bands having maxima at 376 nm (band II) and 720 nm (band I).

Crystallographic Studies. For all of the complexes, X-ray diffraction intensity data were measured at 150(1) K on a Bruker SMART APEX CCD-based diffractometer system (Mo Kα radiation, $\lambda = 0.71073$ Å).[13] Raw data frame integration and Lorentz-polarization corrections were performed with SAINT+.[13] Analysis of the data showed negligible crystal decay during collection. Direct methods structure solution, difference Fourier calculations, and full-matrix least-squares refinement against F^2 were performed with SHELXTL.[14] All non-hydrogen atoms were refined with anisotropic displacement parameters. Details of the data collection are given in Table 1, while further details regarding the solution and refinement of the structures follow below.

Final unit cell parameters of compound **1** were determined by least-squares refinement of 5951 strong reflections from the data set. The asymmetric unit consists of half of one $Cu_2(L_{C2})_4(py)_2$ complex residing on a crystallographic inversion center, one CH_2Cl_2 molecule, and half of a CH_3OH molecule, which is disordered about an inversion center. Hydrogen atoms, except for those of the CH_3OH group, were located in difference maps before being placed in geometrically idealized positions and included as riding atoms. Hydrogen atoms could not be located and were not calculated for the disordered CH_3OH.

Final unit cell parameters of compound **2** were determined by least-squares refinement of 6311 strong reflections from the data set. The asymmetric unit consists of half of one $Cu_2(L_{C3})_4(py)_2$ complex residing on a crystallographic inversion center and one CH_2Cl_2 molecule. Hydrogen atoms were located in difference maps before being placed in geometrically idealized positions and included as riding atoms.

There was no observable high-angle X-ray scattering of compound **3** due to the small crystal size and the presence of disorder in the crystal. The data were truncated at $2\theta = 45°$ for this reason. Final unit cell parameters were determined by least-squares refinement of 3029 strong reflections from the data set. The asymmetric unit consists of one copper atom, two L_{C2} ligands, and half of a 4,4-bipyridine ligand located on a 2-fold axis of rotation. The $Cu_2(L_{C2})_4$ core of the compound is also located on a C_2 axis. There is a region of disordered solvent molecules in the crystal which could not be modeled satisfactorily. Trial modeling attempts indicated a mixture of CH_2Cl_2 and CH_3OH. The program Squeeze (Platon)[15] was used to remove the contribution of these diffusely scattering species from the structure factor calculations. The program calculated a solvent-accessible region of 857.3 Å^3 per unit cell (13.4% of the total unit cell volume). The reported FW, F(000), and d_{calcd} reflect known unit cell contents only. Hydrogen atoms were placed in geometrically idealized positions and included as riding atoms.

Final unit cell parameters of compound **4** were determined by least-squares refinement of 9495 strong reflections from the data set. The asymmetric unit consists of one Cu atom, two L_{C3} ligands, and half of a 4,4′-bipyridine molecule. The 4,4′-bipyridine group is situated about a crystallographic inversion center. Another inversion center generates a $Cu_2(L_{C3})_4$ unit. There are also one methanol molecule of crystallization and a region of disordered dichloromethane molecules in the asymmetric unit. The dichloromethane disorder was modeled with five independent CH_2Cl_2 molecules of variable occupancy. A total of 15 C−Cl and Cl−Cl distance restraints were used for the disordered species. Site occupation factors for each CH_2Cl_2 group were refined, resulting in the final reported composition. Non-hydrogen atoms were refined with anisotropic displacement parameters, except for some of the disordered CH_2Cl_2 groups, which were refined isotropically. Hydrogen atoms were placed in geometrically idealized positions and included as riding atoms. The largest residual electron density peaks remained in the vicinity of the CH_2Cl_2 disorder, indicating the approximate nature of the disorder model and solvent composition of the crystal.

Results

Synthesis. The protonated ligands were prepared in a one-pot reaction between 1,8-naphthalic anhydride and the corresponding amino acids in dimethylformamide (Scheme 2). The ligands formed as white solids after precipitation with ice and cold water and were isolated by filtration. Both *N*-(3-propanoic acid)-1,8-naphthalimide (HL_{C2}) and *N*-(4-butanoic acid)-1,8-naphthalimide (HL_{C3}) have only limited solubility in organic solvents, an indication of strong π−π interactions between the naphthalimide moieties and hydrogen bonds between the carboxylic groups. These compounds have been prepared previously by a similar route for use in medicinal studies[16] but do not appear to have been used previously in the syntheses of coordination complexes.

(13) *SMART*, version 5.625; *SAINT+*, version 6.22; *SADABS*, version 2.05; Bruker Analytical X-ray Systems, Inc.: Madison, WI, 2001.

(14) Sheldrick, G. M. *SHELXTL*, version 6.1; Bruker Analytical X-ray Systems, Inc.: Madison, WI, 2000.

(15) SQUEEZE: Sluis, P. v. d.; Spek, A. L. *Acta Crystallogr., Sect. A* **1990**, *46*, 194−201. *PLATON*; Spek, A. L., Ed.; Utrecht University: Utrecht, The Netherlands, 1998.

(16) (a) Chapman, J. M.; Wyrick, S. D.; Maguire, J. H.; Cocolas, G. H.; Hall, I. H. *Pharm. Res.* **1984**, *1*, 267. (b) Hall, I. H.; Chapman, J. M.; Voorstad, P. J.; Cocolas, G. H. *J. Pharm. Sci.* **1984**, *73*, 956.

Table 1. Selected Crystal Data and Structure Refinement for $[Cu_2(\mathbf{L_{C2}})_4(py)_2]\cdot 2(CH_2Cl_2)\cdot(CH_3OH)$ (**1**), $[Cu_2(\mathbf{L_{C3}})_4(py)_2]\cdot 2(CH_2Cl_2)$ (**2**), $[Cu_2(\mathbf{L_{C2}})_4(bipy)]\cdot$unknown solvate (**3**), and $[Cu_2(\mathbf{L_{C3}})_4(bipy)]\cdot(CH_3OH)_2\cdot(CH_2Cl_2)_{3.37}$ (**4**)

	1	**2**	**3**	**4**
formula	$C_{73}H_{58}Cl_4Cu_2N_6O_{17}$	$C_{76}H_{62}Cl_4Cu_2N_6O_{16}$	$C_{70}H_{48}Cu_2N_6O_{16}$	$C_{79.37}H_{70.74}Cl_{6.74}Cu_2N_6O_{18}$
fw	1560.13	1584.20	1356.22	1762.79
cryst syst	triclinic	triclinic	orthorhombic	monoclinic
space group	$P\bar{1}$	$P\bar{1}$	*Pbcn*	$P2_1/n$
T (K)	150(1)	150(1)	150(1)	150(1)
a, Å	10.3790(5)	10.3864(4)	13.9745(6)	13.9313(5)
b, Å	12.0345(6)	12.7283(5)	26.8970(12)	22.1401(8)
c, Å	14.4327(7)	14.2234(6)	17.0340(8)	14.2574(5)
α, deg	91.8070(10)	105.6330(10)	90	90
β, deg	108.7970(10)	93.8260(10)	90	117.6210(10)
γ, deg	101.0450(10)	108.8280(10)	90	90
V, Å^3	1666.51(14)	1689.36(12)	6402.6(5)	3896.4(2)
Z	1	1	4	2
R_1, $I > 2\sigma(I)$	0.0434	0.0350	0.0468	0.0549
wR_2, $I > 2\sigma$(I)	0.1128	0.0805	0.0884	0.1437

Scheme 2. Preparation of $\mathbf{HL_{C2}}$ and $\mathbf{HL_{C3}}$

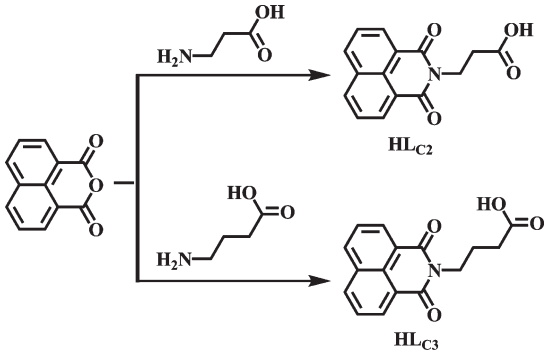

The reaction of these carboxylic acids with $Cu_2(O_2CCH_3)_4(H_2O)_2$ was carried out using the layering method in the presence of a base, and either pyridine (py) or 4,4′-bipyridine (bipy) as the axial ligand. Onto the dichloromethane solution of $\mathbf{HL_{C2}}$ or $\mathbf{HL_{C3}}$ and pyridine or 4,4′-bipyridine was layered pure methanol, and then a methanol solution of $Cu_2(O_2CCH_3)_4(H_2O)_2$ was added as the third layer. After a few days, blue or green X-ray-quality crystals of $[Cu_2(\mathbf{L_{C2}})_4(py)_2]\cdot 2(CH_2Cl_2)\cdot(CH_3OH)$ (**1**), $[Cu_2(\mathbf{L_{C3}})_4(py)_2]\cdot 2(CH_2Cl_2)$ (**2**), $[Cu_2(\mathbf{L_{C2}})_4(bipy)]\cdot$unknown solvent (**3**), and $[Cu_2(\mathbf{L_{C3}})_4(bipy)]\cdot(CH_3OH)_2\cdot(CH_2Cl_2)_{3.37}$ (**4**) were obtained. In the cases of **1** and **2**, the added base was pyridine, which is also a reactant, and therefore was added in excess. In the cases of **3** and **4**, the base was NEt_3, and only a slight excess of 4,4′-bipyridine was added to the reaction mixture. The products are insoluble materials. The reflectance spectra of all four compounds show two bands characteristic to Cu(II) paddlewheel complexes having maxima in the ranges 371−384 nm (band II) and 714−753 nm (band I).

Solid State Structure Analysis. Selected bond lengths and angles are gathered in Table 2. In all cases, at the core of these four compounds lies the square $Cu_2(O_2CR)_4$ "paddlewheel" SBU structural motif. The nonbonding Cu···Cu distances average 2.66 Å. The orientation of the naphthalimide arms is a function of the length of the link between the carboxylate and the 1,8-naphthalimide group.

Figure 1 shows an ORTEP diagram for $[Cu_2(\mathbf{L_{C2}})_4(py)_2]\cdot 2(CH_2Cl_2)\cdot(CH_3OH)$ (**1**). Four carboxylic groups from four separate ligands bridge the two copper(II) atoms. In addition, one pyridine molecule completes the remaining coordination site on the Cu(II) metallic center. When observed along the py−Cu−Cu−py axis (see Figure 2a), for each SBU there are two pairs of ligands with different orientations of the alkyl spacers: one is almost linear, while the second is bent at approximately 60°. As shown, all naphthalimide moieties participate in $\pi-\pi$ stacking interactions, with the dipole vectors of the 1,8-naphthalimide groups oriented at 180°. While there are no criteria to prefer one interaction over the other, since they both have the same characteristics, for ease of description, it will be considered that the $\pi-\pi$ stacking interactions formed by the "linear" ligand generate chains along the body diagonal of the unit cell, while the interactions formed by the "bent" ligand assemble the chains into sheets, yielding an overall two-dimensional arrangement of the $Cu_2(O_2CR)_4$ SBUs, solely organized by noncovalent forces. The distance between the rings for the linear ligands is 3.38 Å, whereas for the bent ligands, it is 3.52 Å. In both cases, the rings are exactly parallel. Figure 2b shows a view down the chain of the same sheet; in this orientation, the stacking of the "bent" ligands lies

Table 2. Selected Bond Lengths (Å) and Angles (deg) for **1**−**4**

	1	**2**	**3**	**4**
		Bond Distances		
Cu(1)−O(7)	1.9634(19)	1.9706(16)	1.915(3)	1.967(3)
Cu(1)−O(4a)	1.9639(18)	1.9770(15)	2.039(3)	1.968(3)
Cu(1)−O(8a)	1.9722(19)	1.9666(16)	2.054(3)	1.967(2)
Cu(1)−O(3)	1.9769(18)	1.9730(16)	1.915(3)	1.988(3)
Cu(1)−N(3)	2.164(2)	2.1796(18)	2.120(3)	2.150(3)
Cu(1)−Cu(1a)	2.6572(6)	2.6632(5)	2.6870(9)	2.6147(8)
		Bond Angles		
O(7)−Cu(1)−O(4a)	89.40(8)	90.04(7)	88.50(14)	88.13(12)
O(7)−Cu(1)−O(8a)	167.07(8)	167.47(6)	85.36(14)	168.44(10)
O(4a)−Cu(1)−O(8a)	86.66(8)	88.72(7)	156.67(12)	89.15(11)
O(7)−Cu(1)−O(3)	88.06(8)	88.57(7)	174.35(14)	90.69(12)
O(4a)−Cu(1)−O(3)	167.66(8)	167.50(6)	95.14(11)	168.76(10)
O(8a)−Cu(1)−O(3)	93.18(8)	89.95(7)	89.61(14)	89.80(11)
O(7)−Cu(1)−N(3)	101.36(9)	96.80(7)	92.38(14)	98.17(11)
O(4a)−Cu(1)−N(3)	100.28(8)	95.21(6)	101.25(13)	100.38(11)
O(8a)−Cu(1)−N(3)	91.46(8)	95.72(7)	101.48(14)	93.37(11)
O(3)−Cu(1)−N(3)	92.06(8)	97.28(7)	91.15(14)	90.85(10)
O(7)−Cu(1)−Cu(1a)	87.33(6)	83.34(5)	89.58(10)	87.47(8)
O(4)−Cu(1)−Cu(1a)	88.58(6)	84.18(4)	80.08(8)	87.75(8)
O(8a)−Cu(1)-Cu(1a)	80.28(6)	84.14(5)	77.39(9)	81.21(7)
O(3)−Cu(1)−Cu(1a)	79.25(6)	83.32(5)	86.80(9)	81.03(7)
N(3)−Cu(1)−Cu(1a)	167.57(7)	179.38(5)	177.66(12)	170.20(8)

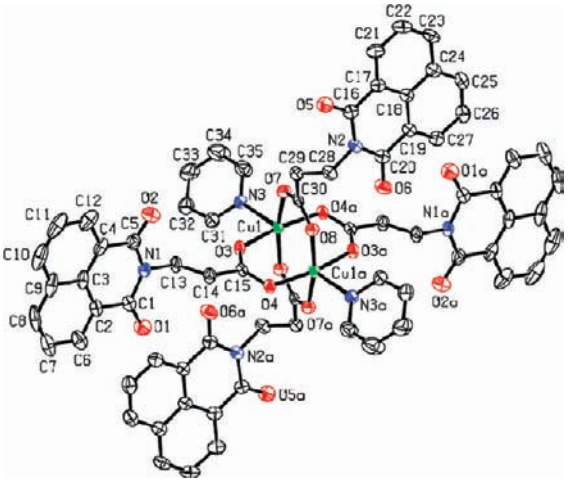

Figure 1. ORTEP diagram of $[Cu_2(\mathbf{L_{C2}})_4(py)_2]\cdot 2(CH_2Cl_2)\cdot(CH_3OH)$ (**1**). Solvent molecules not shown.

in the middle of the picture. The pyridine molecules are situated on top of and below the sheets.

As shown in Table 3, we have defined a parameter that relates the amount of slippage one ring involved in the $\pi-\pi$ stack has with respect to the other. The parameter (χ) is a composite number that takes into account both slippage along the direction of the naphthalimide dipole vectors and slippage at right angles to the vectors (sideways), both of which are observed. The value is (Figure 3) the third side of the right triangle (red line) formed with the average perpendicular distance (green line) between the rings and the line joining the central carbon atoms (C3 and C18 in this case, blue line) of the two rings. For **1**, as can be seen in Figure 2, the naphthalimide groups in the chain direction have mainly sideways slippage of the vectors with χ = 1.64 Å, whereas for the sheet direction, the groups are nearly exactly centered on top of each other with no sideways slippage, giving χ = 0.62 Å.

A third type of $\pi-\pi$ stacking arranges the sheets into a three-dimensional structure, as shown in Figure 4, where three layers, in the same orientation as pictured in Figure 2b, are shown. The interaction is between the "chain"- and "sheet"-type naphthalimide groups from different layers with the dipole vectors oriented at 141°; the distances between the naphthalimide rings is 3.44 Å and χ = 1.17 Å. Interestingly, the axial pyridine groups do not interfere with this interaction and reside in the pockets between the stacked naphthalimide groups. The closest Cu···Cu nonbonding, interdimer distance is in this direction at 8.51 Å, within the sheets the shortest distances are longer at 14.8 and 18.5 Å

The ORTEP diagram of $[Cu_2(\mathbf{L_{C3}})_4(py)_2]\cdot 2(CH_2Cl_2)$ (**2**) is shown in Figure 5. The central $Cu_2(O_2CR)_4$ "paddlewheel" core remains essentially unchanged, but the presence of an extra CH_2 within the alkyl chain linking the carboxylate and naphthalimide groups provides enough flexibility to arrange two naphthalimide moieties one on top of the other rather than retain the "square" architecture imposed by the SBU core. Each SBU unit of **2** has a double cleft shape which is self-complementary to others with each end interacting with the end of another, forming chains that run along the body diagonal of the unit cell

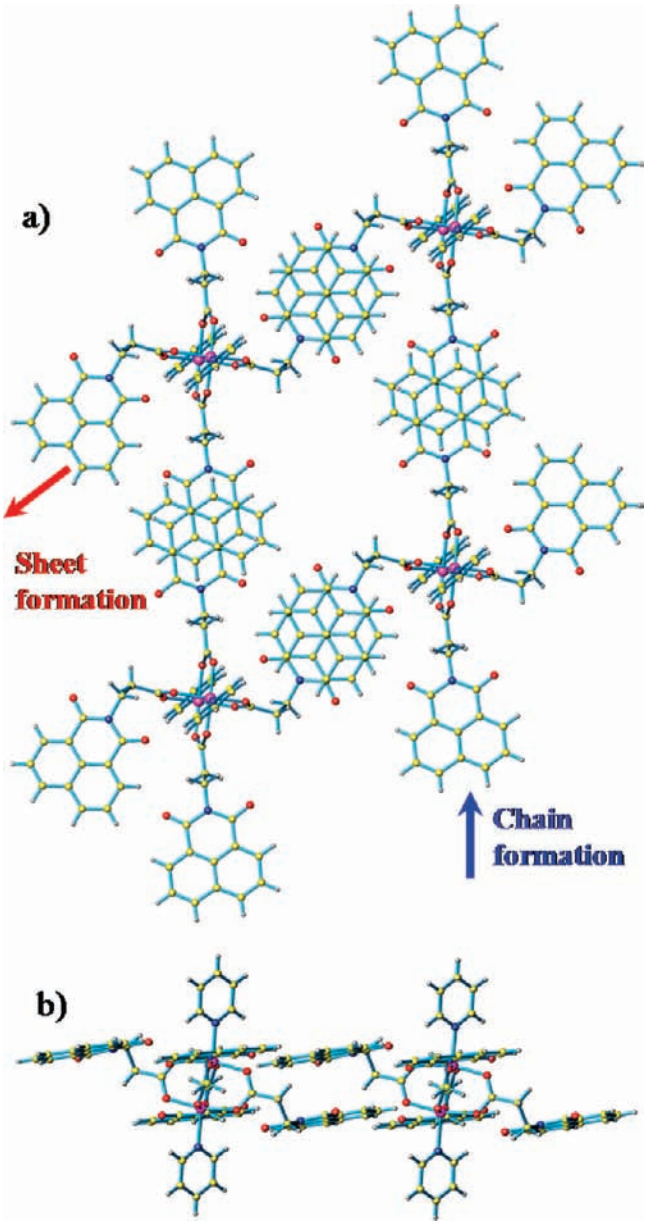

Figure 2. (a) The two-dimensional structure of **1** observed along the py−Cu−Cu−py axis. Each type of naphthalimide group contributes to the growth of the network in one direction, as indicated by the blue and red arrows, respectively. (b) View down the chain of the sheet shown in part a. Color code: copper, purple; carbon, yellow; oxygen, red; nitrogen, blue; hydrogen, gray.

(Figure 6, left to right, three chains shown). These chains are arranged in sheets by additional $\pi-\pi$ stacking of the "outside" naphthalimide units that overlap to form the chains. As with **1**, the pyridine molecules are situated above and below the sheets. In contrast to **1**, there is no organizing feature that binds the sheets into a 3-D structure. In **1** the naphthalimide groups are parallel to the sheets and can interact with the next sheet, whereas in **2** they are perpendicular to the sheets.

The three types of $\pi-\pi$ stacking interactions of the naphthalimide units have different interaction parameters. There are two types of interactions between each end of the molecules forming the "chain" direction: two "outer" interactions in each case with distances between the rings of 3.32 Å and one "inner" interaction where the

Table 3. 1,8-Naphthalimide Interaction Parameters

compound	ring type	central carbon− central carbon distance (Å)	dipole angle (deg)	plane angle (deg)	av. perpendicular distance (Å)	av. slippage, χ (Å)
1	chain	3.76	180	0.0	3.38	1.64
	sheet	3.58	180	0.0	3.52	0.62
	intersheet	3.64	141	3.1	3.44	1.17
2	chain	3.59	169	3.5	3.32	1.35
	chain	4.44	180	0.0	3.40	2.86
	interchain	3.95	180	0.0	3.40	2.01
3	ribbon	3.91	180	0.0	3.60	1.52
	ribbon	3.96	134	6.7	3.68	1.45
	interribbon	4.57	68	6.4	3.52	2.90
4	inter	3.74	86	2.3	3.41	1.54
	intra	3.80	35	5.4	3.42	1.66

perpendicular distance is 3.40 Å. The two "outer" interactions have the dipole vectors of the naphthalimide units oriented at 169° with χ = 1.35 Å, whereas the "inner" interaction, although oriented at 180°, is significantly slipped with χ = 2.86 Å, indicating a weaker interaction.

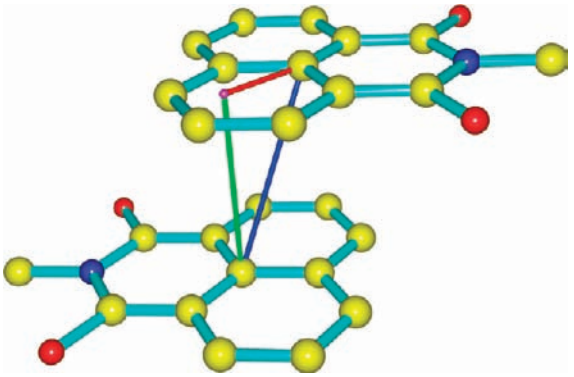

Figure 3. The slippage parameter χ, shown as the red line. The green line is the perpendicular distance between the rings and blue line is the distance between the two ring central carbon atoms.

Figure 7a,b shows the view of the two interactions perpendicular to the naphthalimide planes. While both have sideways slippage, it is much larger in the case of the inner interaction (Figure 7b), but still some interaction is evident. Table 3 shows that the interchain interaction is oriented at 180° with a perpendicular distance between the rings of 3.40 Å and χ = 2.01 Å. As can be seen in Figure 7c, in this case, χ is intermediate between the other two interactions. In this structure, the closest Cu···Cu nonbonding, interdimer distance is between the chains at 13.6 Å.

The ORTEP diagram of $[Cu_2(\mathbf{L_{C2}})_4(bipy)]$ (**3**) is shown in Figure 8. The asymmetric unit consists of one copper atom, two $\mathbf{L_{C2}}$ ligands, and half of a 4,4-bipyridine ligand located on a 2-fold axis of rotation. The $Cu_2(\mathbf{L_{C2}})_4$ core of the compound is also located on a C_2 axis. The program Squeeze (Platon) was used to remove diffusely scattering

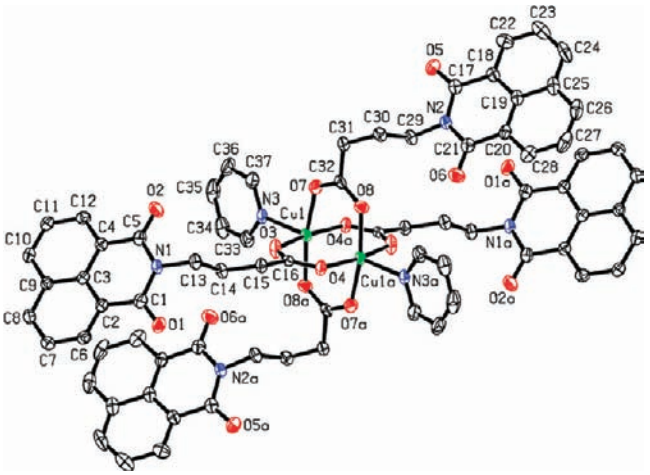

Figure 5. ORTEP diagram of $[Cu_2(\mathbf{L_{C3}})_4(py)_2]\cdot 2(CH_2Cl_2)$ (**2**). Solvent molecules not shown.

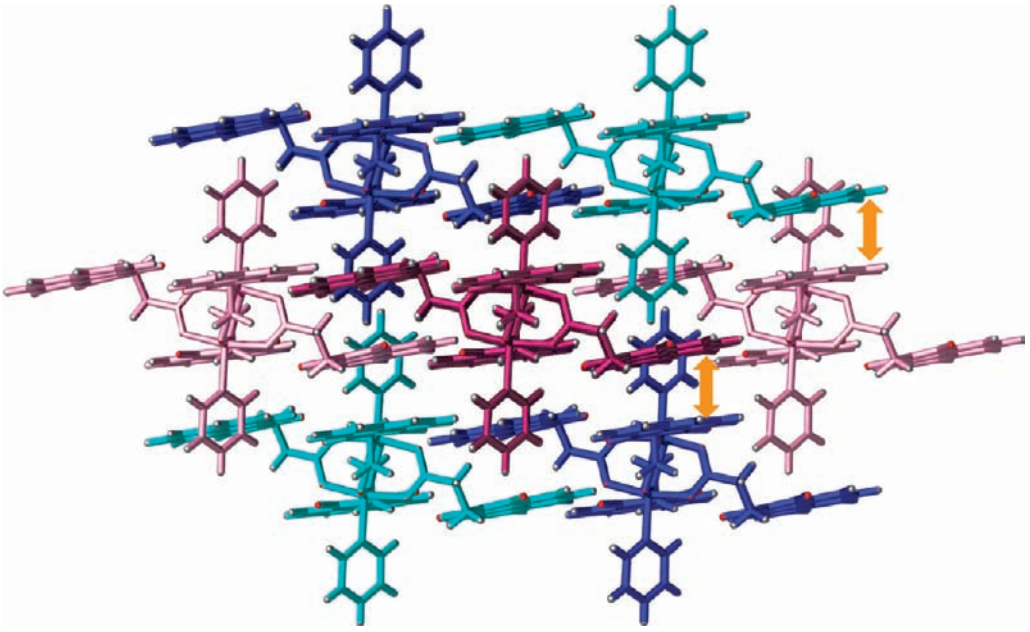

Figure 4. The three-dimensional structure of **1** down the "chain" axis. Blue and red colors delineate each sheet, light and dark colors each dimer in the sheet. Two of the numerous intersheet $\pi-\pi$ stacking interactions are indicated by the orange double arrows.

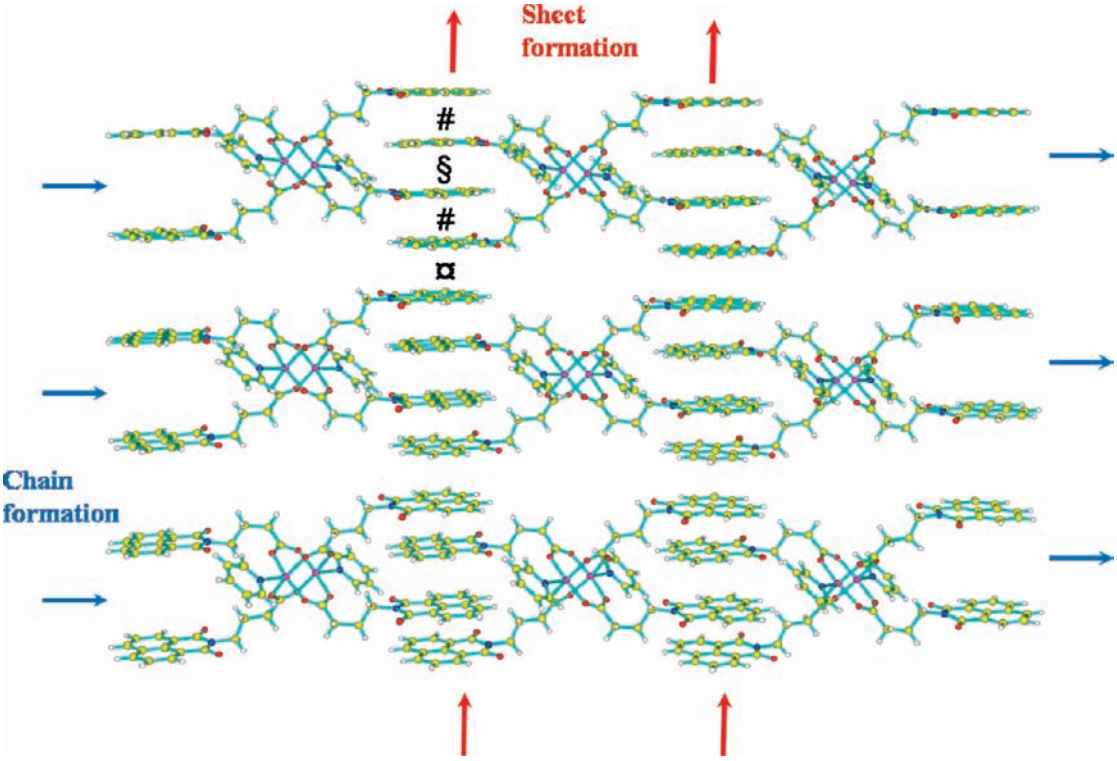

Figure 6. Sheet structure for **2**. The # symbol marks a pair of "outer", the § symbol one "inner", and the ¤ symbol one interchain naphthalimide $\pi-\pi$ interaction.

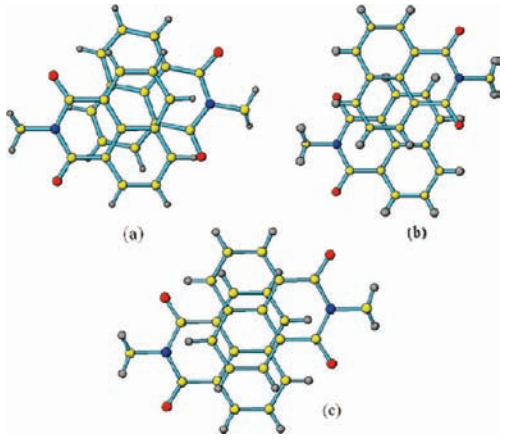

Figure 7. Perpendicular view of the three types of $\pi-\pi$ stacking arrangements for **2**: (a) "outer" interaction in chain direction, (b) "inner" interaction in chain direction, and (c) interchain interaction.

species from the structure factor calculations (13.4% of the total unit cell volume).

The copper(II) core for **3** is the same structural motif as for **1** and **2**. These SBUs are linked by covalent bonds into a one-dimensional chain by the 4,4′-bipy ligands (Figure 9). Although the naphthalimide side arms are approximately arranged in the square shape imposed by the SBU, the $Cu_2(\mathbf{L_{C2}})_4$ SBUs are held together only in a second dimension into one-dimensional ribbons (Figure 10) by two different types of π-stacking interactions. In this ribbon, there are two parallel rows of $Cu_2(\mathbf{L_{C2}})_4$ units. Between the two rows are two of the naphthalimide groups in each SBU involved in a $\pi-\pi$ stacking interaction with a 180° orientation of the dipole vectors (see the middle of Figure 10), a perpendicular

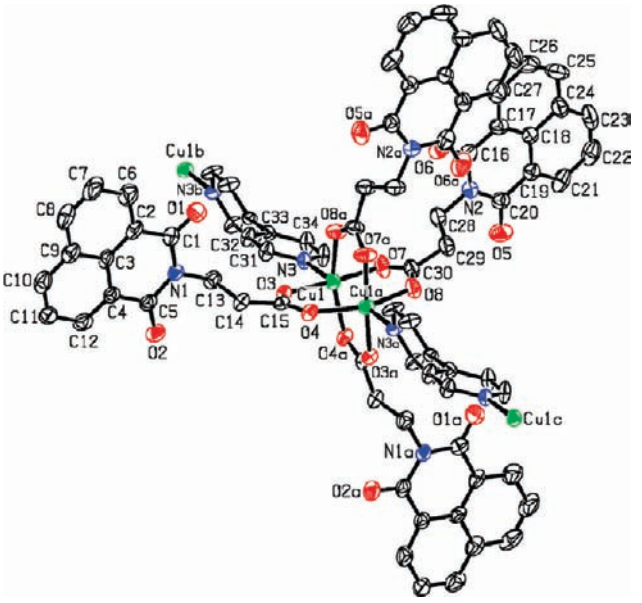

Figure 8. ORTEP diagram of $[Cu_2(\mathbf{L_{C2}})_4(bipy)]\cdot$unknown solvent (**3**). Solvent molecules not shown.

distance of 3.60, and χ = 1.52 Å. The other two naphthalimide groups undergo a different type of $\pi-\pi$ stacking on the outside of the SBU rows, with another equivalent moiety, which also supports the two rows of SBU units within the ribbon. In this case, the naphthalimide groups have their dipole vectors skewed at 134°, a perpendicular distance of 3.68 Å, and χ = 1.45 Å.

These wide and thick ribbons are connected by the 4,4′-bipy groups (Figure 11). If we consider only the ribbons formed by the noncovalent $\pi-\pi$ stacking interactions and

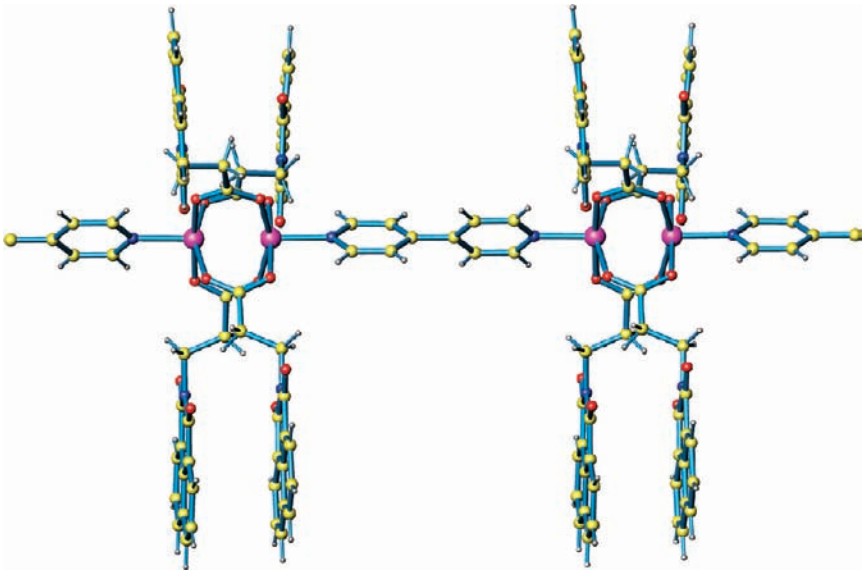

Figure 9. Two dimeric copper units in **3** bridged by a bipyridine molecule.

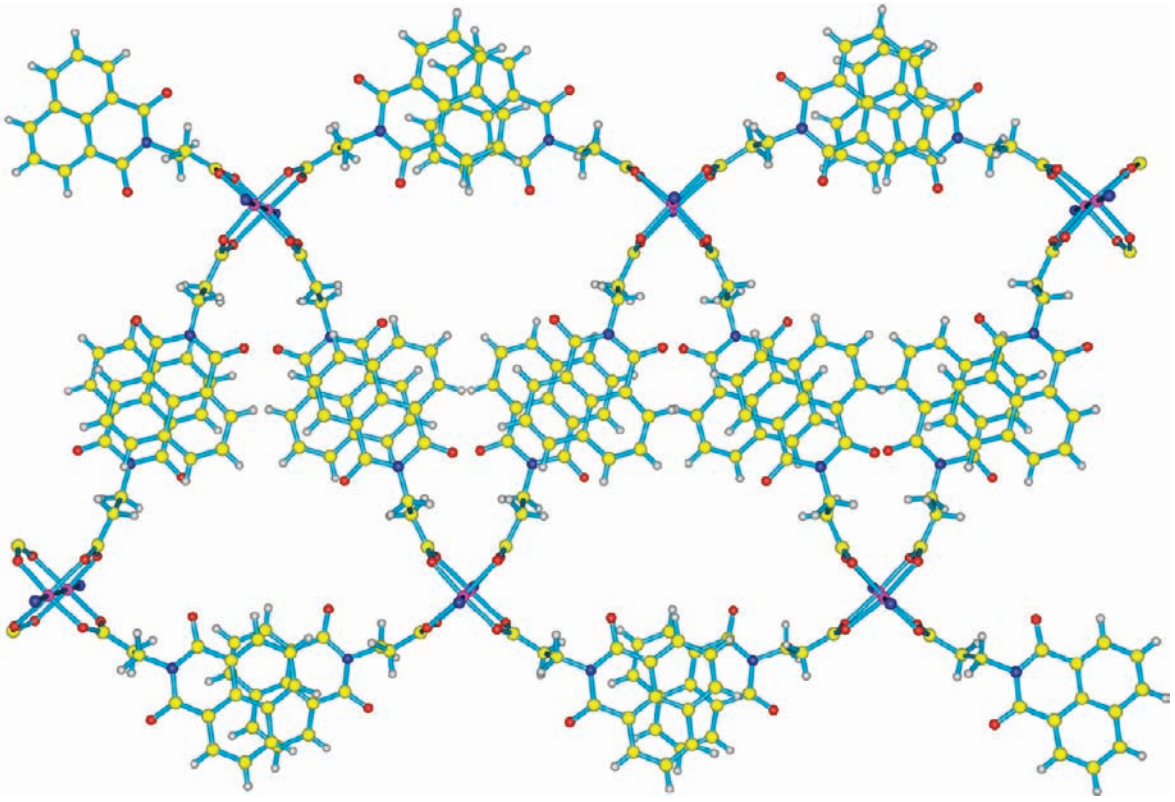

Figure 10. Formation of one-dimensional ribbons in **3** showing the two different types of $\pi-\pi$ stacking that built up the one-dimensional supramolecular structure. Only the nitrogen atoms from the bipy are shown.

covalent 4,4′-bipy ligand pillars, the overall structure of **3** has an infinite two-dimensional double columnar architecture, with large void spaces within them.

In the third dimension, these linked two-dimensional grids are interpenetrating, forming an infinite three-dimensional polycatenated framework. In Figure 12, the red line represents only the $\pi-\pi$ stacking interactions that have the dipole vectors oriented at 180°, and the blue line represent the 4,4′-bipy pillars. The $Cu_2(O_2C)_4$ core is linked into a two-dimensional double-columnar architecture by the strong $\pi-\pi$ stacking interaction of the naphthalimide groups and by 4,4′-bipyridine ligands. This double columnar architecture is interpenetrated at both of its lateral sides by other double-columnar constructions, forming a three-dimensional structure.

Figure 12 does not show the naphthalimide groups that overlap at 120°. Figure 13 shows a different representation from the same direction that includes these rings, where the light and dark red and blue coloring indicate four complete (dark) or half interpenetrating units.

As can be seen by the blue color-coded rings in the column indicated by the arrow, the pairs of naphthalimide groups that overlap at 120° are sideways to each other (in this column, the dark blue rings from the units to the left are in front of and block the light blue rings from the half units to the right). There are $\pi-\pi$ stacking interactions between the red and blue units, in this column, between these blue rings and the "red" 180° overlapping rings above and below them. Only one of the blue 120° rings overlaps in each area, with a vector angle of only 68°, a perpendicular distance of 3.52 Å, and χ = 2.90 Å, values that indicate a weak interaction. The metrics of the blue rings that do not interact are a vector angle = 120°, a perpendicular distance of 3.09 Å, and χ = 6.30 Å, showing the value of the slippage parameter χ. The closest Cu···Cu nonbonding, interdimer distance is in the bipy-linked direction at 11.3 Å; other distances are longer than 17.0 Å.

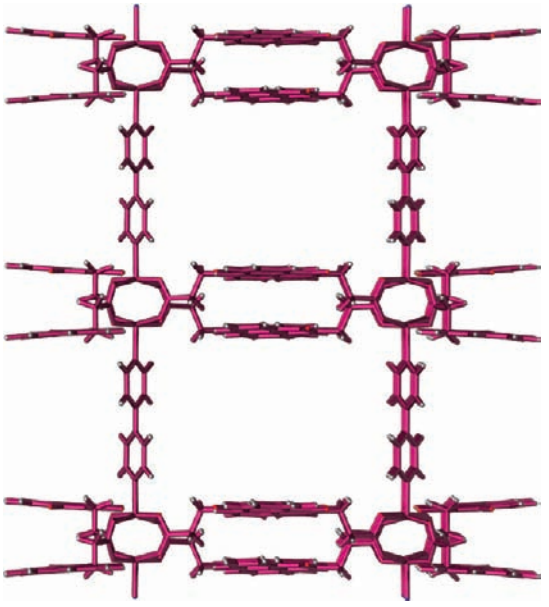

Figure 11. The double columnar architecture of **3** formed by the strong $\pi-\pi$ stacking interaction of the naphthalimide groups and by the covalent bonds of the 4,4′-bipyridine ligands.

An ORTEP diagram of $[Cu_2(\mathbf{L_{C3}})_4(bipy)]\cdot(CH_3OH)_2\cdot(CH_2Cl_2)_{3.37}$ (**4**) is shown in Figure 14. As in the previous compounds, the "paddlewheel" motif of the SBU is present in **4**. Figure 15 pictures two such copper(II) units linked by one 4,4′-bipy molecule, forming a one-dimensional, covalently linked chain. The naphthalimide groups of $\mathbf{L_{C3}}$ in **4** are again situated one on top of the other, as in **2**, but at a much closer distance due to a significant *intramolecular* skewed $\pi-\pi$ stacking interaction. The perpendicular distance between the naphthalimide rings is 3.42 Å and χ = 1.66 Å; because the interaction is intramolecular, the dipole vectors are oriented at a low angle of 35°. In addition to the *intramolecular* $\pi-\pi$ stacking, each of the four naphthalimide units in a SBU is involved in an *intermolecular* $\pi-\pi$ stacking interaction with four different neighboring units (Figure 16) at a distance of 3.41 Å with χ = 1.54 Å. Although intermolecular, the dipole angle is low at 86°. These additional interactions build up a two-dimensional corrugated sheet network.

The 4,4′-bipyridine moieties link these sheets into a three-dimensional framework (Figure 17). The red lines represent the $\pi-\pi$ stacking of the naphthalimide moieties, and the blue lines represent the bipyridine molecules. The sheets formed by the $\pi-\pi$ stacking are parallelly positioned and linked in the third direction by the "pillars". As with **3**, the closest Cu···Cu nonbonding, interdimer distance is in the bipy-linked direction at 11.4 Å, with the through naphthalimide distances being 12.6 Å.

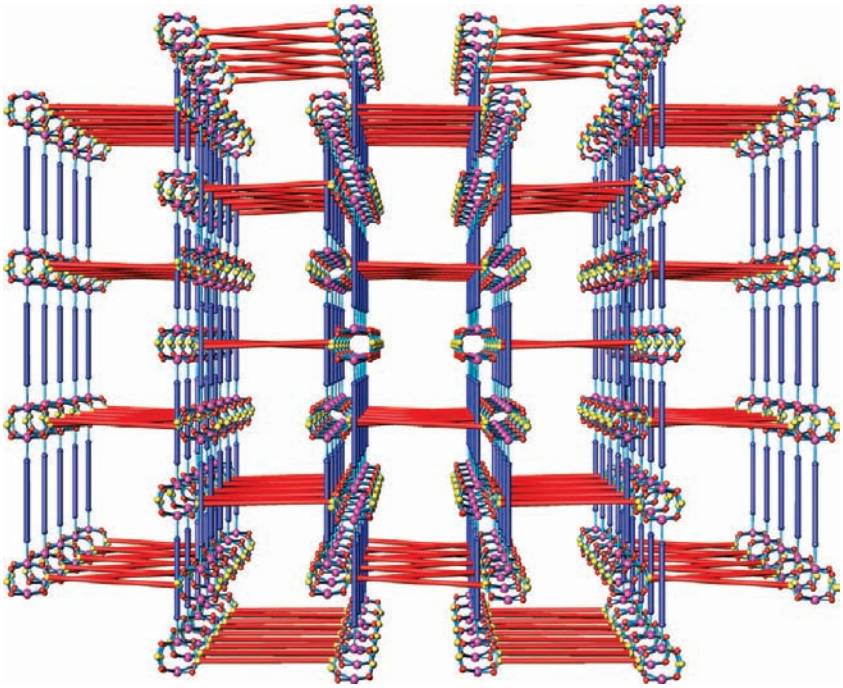

Figure 12. Schematic representation of the polycatenated (interpenetrated) three-dimensional overall structure of **3**. The red lines represent the $\pi-\pi$ stacking of the naphthalimide moieties and the blue lines the bipyridine molecules.

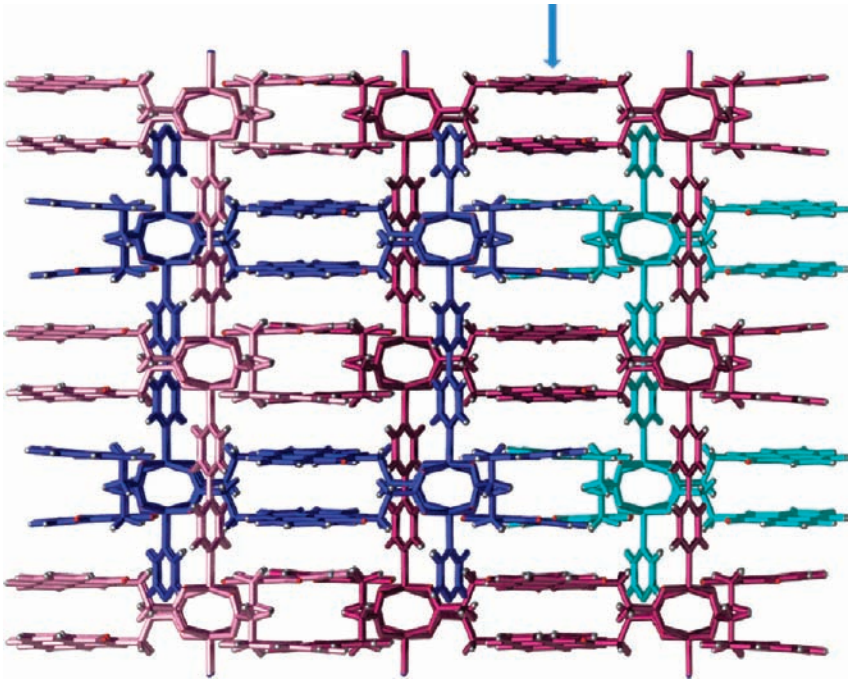

Figure 13. Four interpenetrating double columnar units of **3**, colored dark and light (only half of these units shown), red and blue.

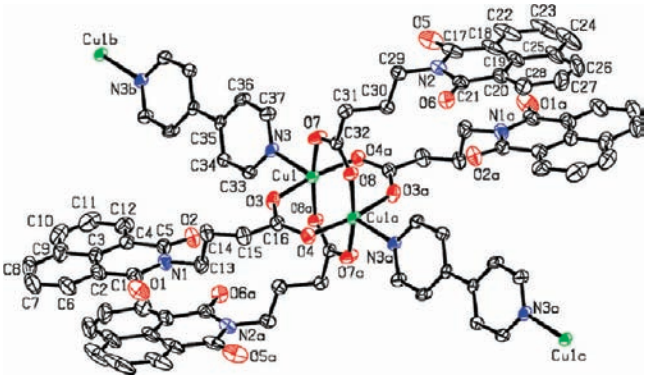

Figure 14. ORTEP diagram of $[Cu_2(\mathbf{L_{C3}})_4(bipy)]\cdot(CH_3OH)_2\cdot(CH_2Cl_2)_{3.37}$ (**4**). Solvent molecules not shown.

SBU Core Geometry. The stereochemistry of the copper centers in the four complexes can be determined by the Addison τ factor, a parameter that describes the distortion from the square pyramidal to trigonal bipyramidal geometry.[17] In a regular square pyramid, $\tau = 0$, and for an ideal trigonal bipyramid, $\tau = 1$. For **1**, **2**, and **4**, the coordination environment of the copper centers is nearly a perfect square pyramid with τ factors of 0.010, 0.001, and 0.005; **3** shows a moderate distortion with $\tau = 0.29$.

Magnetic Properties. The magnetic susceptibilities of **1**, **2**, **3**, and **4** were investigated from 4 to 300 K; for compound **2**, the temperature range was extended to 400 K. The magnetic behavior of **2** is illustrated in Figure 18, which shows that the compound *exhibits diamagnetic behavior* in the 5−300 K and 200−400 K ranges. The magnetic properties of the other three compounds were the same. Because of these unusual results, we measured the magnetic properties of the $Cu_2(O_2CCH_3)_4(H_2O)_2$ starting material for our studies, which proved to be paramagnetic at room temperature, showing antiferromagnetic behavior at lower temperatures, with the data matching literature values.[12]

Impact of Rotation of Naphthalimide Groups in $\pi-\pi$ Stacking. We have investigated the orientation dependence of intermolecular interaction energy between naphthalimide rings using the MP2/6-31G* level of theory, with all electrons correlated, using Q-Chem software and custom script files.[18] The rings were constrained to parallel planes separated by 3.5366 Å, which is the energy minimum at this level of theory. The centers of mass of the rings were constrained to be on the axis of rotation, and the hydrocarbon bridge to the carboxylate group was modeled by a methyl group. Surprisingly, the computed energy profile, Figure 19, is relatively insensitive to the angle of rotation, apart from the region of steric interaction of methyl groups, consistent with very recent calculations on polycyclic hydrocarbons.[19] The binding energies are substantial, varying between about 16.5 and 15 kcal/mol, until the dipole vector angle goes under 30°.

Discussion

Four new compounds that combine the robustness and directional orientation of the $Cu_2(O_2CR)_4$ core with the strong $\pi-\pi$ stacking capabilities of the 1,8-naphthalimide synthon were successfully prepared and structurally analyzed.

As expected from the design of the system, the "square" SBU units in **1** and **2** are linked by the $\pi-\pi$ stacking interactions of the 1,8-naphthalimide groups into a two-dimensional sheet structure. The addition of the extra CH_2 group in the alkyl chain of the ligand in **2** greatly influences both the molecular and the supramolecular structures. The semirigidity of $\mathbf{L_{C2}}$ in **1** limits the possible orientations of

(17) (a) Addison, A. W.; Rao, N. T.; Reedijk, J.; van Rijn, J.; Verschoor, G. C. *J. Chem. Soc., Dalton Trans.* **1984**, 1349. (b) Rodiguez-Fortea, A.; Alemany, P.; Alvarez, S.; Ruiz, E. *Chem.—Eur. J.* **2001**, *7*(3), 627.

(18) Shao, Y.; et al. *Phys. Chem. Chem. Phys.* **2006**, *8*, 3172.

(19) Yurtsever, E. *J. Phys. Chem.* **2009**, *113*, 924.

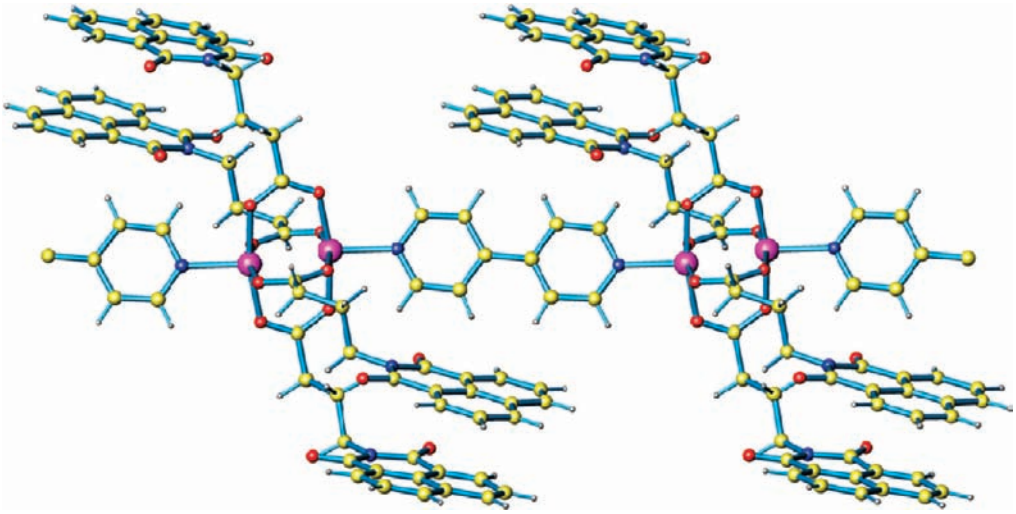

Figure 15. Two $Cu_2(\mathbf{L_{C3}})_4$ dimers connected by a 4,4′-bipy molecule in **4**.

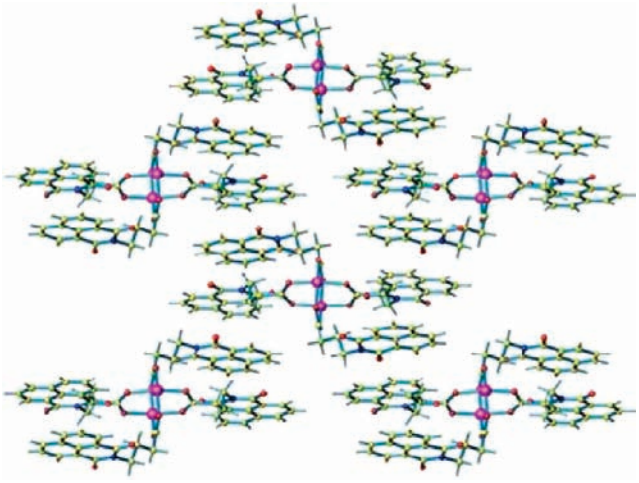

Figure 16. Six $Cu_2(\mathbf{L_{C3}})_4$ units of **4** involved in skewed intermolecular $\pi-\pi$ stacking.

the ligand "arms"; they are fairly coplanar and directed in the four directions implanted by the SBU units (Figure 2). This compels the building blocks to self-assemble into a two-dimensional sheet, based on the $\pi-\pi$ stacking of the naphthalimide moieties in the basically "square" arrangement of the SBU. This arrangement of the naphthalimide groups orients them in positions that can form additional $\pi-\pi$ stacking interactions in the third direction, leading to a three-dimensional overall structure, completely organized by noncovalent forces. The increased flexibility of $\mathbf{L_{C3}}$ allows the arms in **2** to adopt a linear orientation not based on the "square" arrangement of the SBU. The $\pi-\pi$ stacking interactions of the naphthalimide moieties in this structure are different than in **1** (Figure 6), restricting the overall structure to a two-dimensional sheet. In both cases, the pyridine molecules bounded in the axial positions do not appear to influence the overall structures.

Adding linear covalent bonding interactions by changing the axial ligand from pyridine to 4,4-bipyridine leads to three-dimensional structures, as anticipated, but the forces that hold together the three-dimensional structure for **3** were unexpected. While the covalent link of the 4,4′-bipyridine group adds a dimension of connectivity, the $\pi-\pi$ stacking interactions *do not form* the expected two-dimensional sheet, as observed with this ligand in **1**. Instead, the $\pi-\pi$ stacking interactions only lead to one-dimensional ribbons. Despite this difference, **3** has a three-dimensional structure. The third dimension is held together by *mechanical interlocking* that arises from interpenetration of the two-dimensional structure formed by the covalent bonds of the 4,4′-bipyridine linker and noncovalent $\pi-\pi$ stacking interactions. Thus, the *three-dimensional structure of **3** is very unusual in that each of the three directions are held together by different forces*: covalent bonding in the 4,4′-bipyridine direction, robust $\pi-\pi$ stacking interactions of the naphthalimide groups in the second direction, and mechanical interlocking in the third direction.

In the case of **4**, the flexibility of the ligand leads to the only example of *intramolecular* $\pi-\pi$ stacking, but *intermolecular* $\pi-\pi$ stacking leads to the expected sheet structure supported only by the noncovalent interactions. In this case, the use of the linking 4,4-bipyridine axial ligand leads to the expected three-dimensional structure supported by the covalent linker and $\pi-\pi$ stacking.

A number of the naphthalimide $\pi-\pi$ stacking interactions in these four structures are *not* made with the dipole vectors oriented at 180°; skewed stack arrangements are observed. This difference from our earlier work was particularly important in the formation of ribbons rather than sheets in the structure of **3** and the intramolecular interactions in **4**. Our calculations show very little loss in energy on rotation of the rings and indicate that the interaction at all angles of rotation, other than near the point where the dipole vectors are close to parallel, is substantial. For the compounds reported here, the angle ranges from 180 to 68° for intermolecular interactions and is very low at 35° for the one intramolecular interaction, in compound **4**. Both the computed and observed lack of the rotational dependence is likely due to efficient screening of partial charges on the electronegative nitrogen and oxygen atoms by the aromatic π electrons, which reduces the impact of the dipole contributions that are maximized with the dipole vectors oriented at 180°.

In addition to determining the angle of rotation of each interaction, we have determined the perpendicular distance between the rings, the classic indication of the strength of a $\pi-\pi$ stacking interaction (Table 3).[5] The range of this

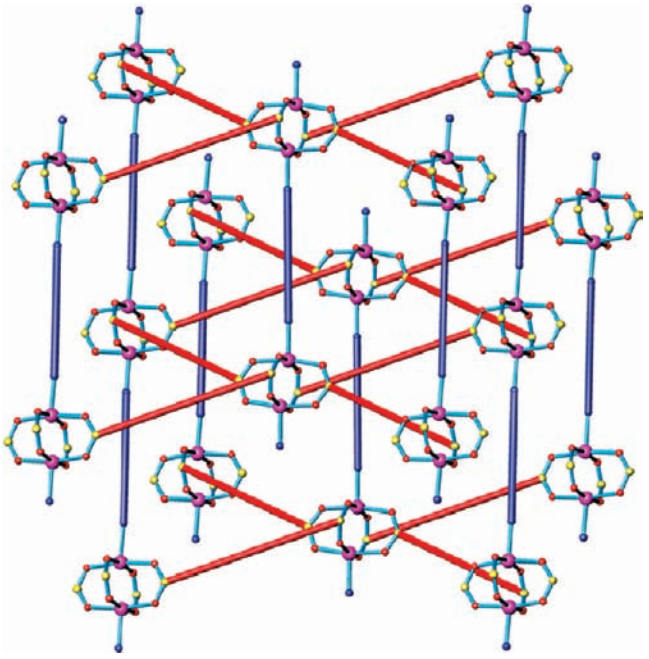

Figure 17. The three-dimensional framework of **4**. The red lines represent the $\pi-\pi$ stacking of the naphthalimide moieties and the blue lines the bipyridine molecules.

parameter is 3.32 to 3.60 Å, distances indicating strong interactions in all cases. The rings are parallel or nearly parallel, even the one case of the intramolecular interaction. A "slippage" distance, χ, a parameter that we have developed to indicate the offset of one ring with respect to the other, also helps define the interaction, as visualized in Figure 7 for the three types of interactions in compound **2**. The parameter ranges from 0.62 Å to 2.90 Å, showing, in conjunction with the large range in the orientation of the dipole vectors, that the 1,8-naphthalimide supramolecular synthon is extremely versatile and flexible. That some slippage is observed in all cases is expected, as a previous search of the CSD database on somewhat similar systems has noted that "near face-to-face π-stacking interaction is a rare phenomenon."[5] From the available χ data,[7] strong interactions appear to range from 0.62 Å to 2.4 Å, although more data are needed. Importantly, although the perpendicular distances between the rings for all of the interactions in Table 3 are in the range of a strong interaction, in two cases, the slippage parameter χ is large, indicating that these two interactions are not as strong as the others in the table. In assessing the strength of the $\pi-\pi$ stacking interactions, all of the parameters in Table 3 need to be considered.

Recent calculations on the "slippage" of polycyclic hydrocarbons, specifically the linear four-ring fused tetracene, indicate that in those systems the minimum energies are achieved with substantial (ca. 1 Å) slippage both along the chain and perpendicular to it.[19] We also point out that, as part of a larger study on the supramolecular chemistry of phthalimide derivatives, including metal complexes,[20] an interesting report on the structures of a number of 1,8-naphthalimide groups *N*-substituted with pyridine or an arene group and their protonated derivatives has appeared

(20) Barooah, N.; Baruah, J. B. *Mini-Rev. Org. Chem.* **2007**, *4*, 292.

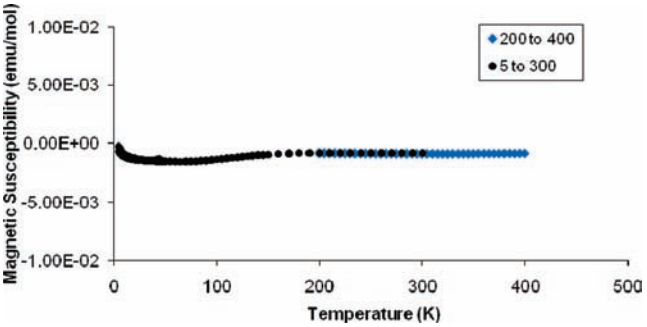

Figure 18. Magnetic susceptibility of **2** from 5 to 300 K and from 200 to 400 K.

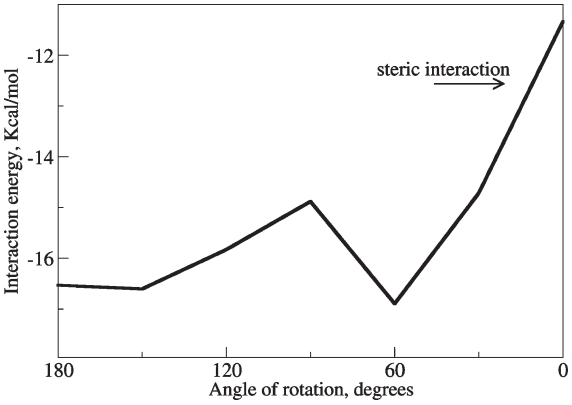

Figure 19. Plot of dipole vector rotation versus energy of the $\pi-\pi$ stacking interaction.

that discusses the relative importance of $\pi-\pi$ stacking when other forces such as hydrogen bonding are present.[21]

The four new structures reported here show that ligand design can lead to supramolecular metal organic framework (SMOF) solids in which the structures are dominated by a combination of covalent bonds and noncovalent $\pi-\pi$ stacking forces. Analogous structures that combine covalent and hydrogen bonding forces have been reported previously.[10,11] Clearly, these types of structures are not as robust as conventional MOF solids held together exclusively by covalent forces but are an important class of organized solids. A particularly attractive feature of building extended structures using ligands containing the 1,8-naphthalimide synthon is the ease of synthesis of the ligand, the condensation of an appropriately substituted amine with 1,8-naphthalic anhydride (Scheme 2).

Complexes that contain the paddlewheel $Cu_2(O_2CCH_3)_4$ building unit are known to possess very strong antiferromagnetic interaction between the unpaired electrons of the Cu(II) centers.[12] This interaction is mediated by superexchange via the four bridging carboxylates and leads to a singlet ground state and a thermally populated triplet excited state.[12] The singlet−triplet energy gap is characterized by the *J* parameter

(21) (a) Sarma, R. J.; Tamuly, C.; Barooah, N.; Baruah, J. B. *J. Mol. Struct.* **2007**, *829*, 29. (b) Barooah, N.; Tamuly, C.; Baruah, J. B. *J. Chem. Sci.* **2005**, *117*, 117.

(22) (a) Bie, H.-Y.; Yu, J.-H.; Zhao, K.; Duan, L.-M.; Xu, J.-Q. *J. Mol. Struct.* **2005**, *741*, 77. (b) Bie, H.-Y.; Yu, J.-H.; Zhao, K.; Duan, L.-M.; Xu, J.-Q. *J. Mol. Struct.* **2006**, *791*, 201. (c) Campbell, G. C.; Haw, J. F. *Inorg. Chem.* **1988**, *27*, 3706. (d) Jotham, R. W.; Kettle, S. F. A.; Marks, J. A *J. Chem. Soc., Dalton Trans.* **1972**, 428. (e) Dalai, S.; Mukherjee, P. S.; Zangrando, E.; Chaudhuri, N. R.; Chaudhuri, L. *J. Chem. Soc., Dalton Trans.* **2002**, 822.

Table 4. Structural Parameters of Carboxylato-Bridged Cu(II) Compounds

compound	Cu−Cu (Å)	Cu−O (basal) (Å)	Cu−L (axial) (Å)	O−C (Å)	Cu−O−C (deg)	O−C−O (deg)	$-J$ (cm^{-1})
$Cu_2(CH_3COO)_4(py)_2$[a]	2.630(3)	1.981(10)	2.126(10)	1.239(18)	123.4(7)	125.1(9)	325
$Cu_2(CH_3COO)_4(py)_2$[b]	2.645(3)	1.955(8)	2.186(8)	1.244(18)	123.4	125.6	
$Cu_2(CH_3COO)_4(2\text{-pic}^c)_2$	2.671	1.975(10)	2.240(12)	1.244(14)	121.7(10)	125.9(14)	318
$[Cu_2(CH_3COO)_4(4,4'\text{-bipy})]_n \cdot DMF$	2.6037(8)	1.969	2.169(3)	1.247	123.45	124.6	
$[Cu_2(fum^d)_2(4,4'\text{-bipy})] \cdot 0.5H_2O$	2.675(1)	1.970	2.144	1.258	123.9	124.1	296
$Cu_2(C_3H_7COO)_4$	2.584(1)	1.961		1.255	123.5	124.6	322
$\{[Cu_2(glu^e)_2(bpmp^f)](H_2O)_4\}_n$	2.6513(7)	1.9697	2.179(2)	1.258	123.63	124.85	283(8)
$[Cu_2(L_{C2})_4(py)_2](CH_2Cl_2)_2(CH_3OH)$ (**1**)	2.6572(6)	1.9691	2.164(2)	1.258	123.06	125.55	
$[Cu_2(L_{C3})_4(py)_2](CH_2Cl_2)_2$ (**2**)	2.6632(5)	1.9718	2.1796(18)	1.258	123.65	125.15	
$[Cu_2(L_{C2})_4(4,4'\text{-bipy})] \cdot$ unknown solvent (**3**)	2.6870(9)	1.9808	2.120(3)	1.257	123.28	125.1	
$[Cu_2(L_{C3})_4(4,4'\text{-bipy})](CH_2Cl_2)_{3.37}(CH_3OH)_2$ (**4**)	2.6147(8)	1.9725	2.150(3)	1.257	123	124.9	

[a] Monoclinic. [b] Orthorhombic. [c] pic = picoline. [d] fum = fumarate. [e] glu = glutarate. [f] bpmp = N,N′-bis(4-pyridyl)piperazine

that expresses the magnitude of the intramolecular exchange interaction. For $Cu_2(O_2CR)_4(L)_2$-type compounds, J is typically about -300 cm^{-1}.[12,22] For complexes with J values of this magnitude, the antiferromagnetic behavior starts to become evident in magnetic studies below ca. 260 K.[12] The magnetic properties of the new compounds **1**−**4** indicate that these SMOF solids organized partially by $\pi-\pi$ stacking interactions can lead to novel materials. All four compounds are very strongly antiferromagnetically coupled; they are diamagnetic Cu(II) solids at temperatures as high as 400 K. The J values must be more negative than -600 cm^{-1}.

The magnitude of the exchange interaction is known to be influenced by several factors, including the stereochemistry of the Cu(II) ions, the bridging mode of the ligand, the bond angles at the bridging atoms, and the copper−bridge ligand bond lengths. Table 4 contains a comparison of the structural parameters of **1**−**4** with related carboxylato-bridged compounds.[12,22] Although, there are slight differences in bond lengths and angles around the copper cores of **1**−**4** and the other tetracarboxylato complexes, these variations do not explain the unusually high J values of the former compounds. In terms of Cu(II) stereochemistry, Rodriguez-Fortea et al.[17] concluded that, for these types of complexes, an increase of the τ parameter (structures closer to trigonal bipyramidal) leads to a decrease of the antiferromagnetic coupling. Although **3**, the only compound with a structure not close to pure square pyramidal, may have a smaller J value compared to **1**, **2**, and **4**, the effect of the structural distortion could not be determined because the triplet excited state is still not populated in any of these complexes in the studied temperature range. The 4,4′-bipy link is not solely responsible for these J values; the entry in the fifth row of Table 4 has such a linkage with $J = -296$ cm^{-1}. Direct interactions between the different copper(II) dimers are ruled out by the long Cu(II)···Cu(II) (shortest 8.51 Å) separations of the SBU units.

To the best of our knowledge, these compounds represent the first examples of copper carboxylate dimers having antiferromagnetic interactions of this magnitude. We consider that the explanation for the unusual magnetic behavior of **1**, **2**, **3**, and **4** lies in the highly organized SMOF structures of these compounds. The mechanism for how the structures impact the magnetic properties is not clear. Clearly, the strong $\pi-\pi$ stacking organizing forces of the naphthalimide group have an important influence on these magnetic properties, much greater than was expected at the start of this investigation. Future studies will explore this issue further.

Conclusion

The strong $\pi-\pi$ stacking interaction of the 1,8-naphthalimide moiety has been utilized into constructing classical paddlewheel $Cu_2(O_2CR)_4(L)_2$ compounds leading to high-dimensionality materials. The use of the 4,4′-bipyridine ligand in conjunction with the 1,8-naphthalimide functional group leads to three-dimensional solids. In the case of $[Cu_2(\mathbf{L_{C2}})_4(bipy)]$, the compound is unique because it is organized in each of its three dimensions by different forces: covalent bonding from the 4,4-bipyridine, robust $\pi-\pi$ stacking interactions of the naphthalimide, and mechanical interlocking. All four structures serve to demonstrate the viability of the 1,8-naphthalimide as a synthon for the self-assembly of supramolecular edifices, in this case, complexes that mix the covalent bonds generally used with MOF solids with weaker, but still substantial, noncovalent forces to form supramolecular MOF solids. Both the domination of the structures by these $\pi-\pi$ stacking interactions and the calculations show that this stacking is a substantial force. These new complexes are all diamagnetic at room temperature, *the first examples of such behavior for* $Cu_2(O_2CR)_4(L)_2$ *compounds*, showing that the new structural features can lead to unusual physical properties.

Acknowledgment. The authors acknowledge with thanks the financial support of the U.S. National Science Foundation through grant CHE-0715559. We thank Elizabeth Foley for help in the magnetic studies and Jacob Horger for help in the determination of the orientation parameters of the naphthalimide rings.

Supporting Information Available: X-ray crystallographic files in CIF format for the structural determinations of **1**−**4**. This information is available free of charge via the Internet at http://pubs.acs.org.